

# Leakage Inductance Design of Toroidal Transformers by Sector Winding

Francisco de León, *Senior Member, IEEE*, Sujit Purushothaman, *Member, IEEE*, and Layth Qaseer

**Abstract**—Toroidal transformers are commonly used in power electronics applications when the volume or weight of a component is at a premium. There are many applications that require toroidal transformers with a specific leakage inductance value. A transformer with a large (or tuned) leakage inductance can be used to eliminate a (series) filter inductor. In this paper, a procedure to control the leakage inductance of toroidal transformers by leaving unwound sectors in the winding is presented. Also, a simple formula is obtained in this paper that can be used to design transformers with a specific leakage inductance value. The leakage inductance formula is expressed as a function of the number of turns, the geometrical dimensions of the toroidal transformer, such as core internal diameter, external diameter, and height, and the angle of the unwound sector. The formula proposed in this paper has been obtained and validated from laboratory experiments and hundreds of three-dimensional finite element simulations. The techniques described in this paper will find applications in the design of transformers that in addition of providing voltage boosting need to double as filters.

**Index Terms**—Leakage inductance, sector winding, toroidal transformers.

## I. INTRODUCTION

TOROIDAL transformers with an enlarged leakage inductance find applications in several power electronics devices that require a transformer with a specified leakage inductance value. For example, a transformer with a large leakage inductance can be used to eliminate a series inductor for filtering or tuning. Among the applications, we can find a number of converters [1]–[4] and electromagnetic noise reduction transformers [5]–[10]. Particular leakage inductance values for transformers are used to distribute the power flow of parallel paths and to limit the short circuit (SC) currents [11].

Tape wound toroidal transformers made with grain-oriented silicon steel are more efficient, smaller, cooler, and emit reduced acoustic and electromagnetic noise when compared with standard transformers built on staked laminations [12]. Toroidal transformers are commonly used in the power supply of audio, video, telecommunications, and medical equipment. These

transformers are finding new applications in small- to medium-size UPS systems and in the lighting industry (especially in halogen lighting). Aircraft have also benefited from the advantages of toroidal transformers [13].

The equations for computing the leakage inductance of E-I transformers at 60 Hz are readily available [14], [15]. Also available are analytical expressions for computing winding losses and leakage inductance for high frequencies [16], [17].

The theory for toroidal transformers is not nearly as advanced as the theory for E-I transformers. This may be because at this moment toroids are restricted to small powers (tens of kilovolt amperes) and low voltages (possibly up to a few kilovolts). In [18] and [19], an analytical study of the losses at high frequency was presented for toroidal inductors, but the leakage inductance was not considered.

Perhaps, due to the complexity of the winding, researchers have preferred numerical solutions such as finite elements [20], [21]. There exists a semiempiric formula for computing the leakage inductance of small toroidal common-mode chokes [22]. However, in all our cases the formula in [22] predicted erroneous values. We should mention that there is a substantial difference in the sizes of our transformers and those in [22].

In [23], an analytical formulation for computing the leakage inductance of toroidal transformers with circular cross-sectional area is derived elegantly from the solution of Maxwell equations. In [23], the toroidal core is opened and elongated to form a linear rod with circular cross-sectional area and Fourier techniques are applied (this is possible because the rod is terminated with magnetic end planes, which are replaced by images on the infinite rod). This works well in [23] because the toroids are very small and the windings, which never overlap, cover only a small portion of the core perimeter. The transformer cores of this paper are much larger and the windings overlap. Additionally, the cores here do not have circular cross sections.

A technique to enlarge the leakage inductance using interwinding spacing and magnetic insets is given in [24]. The technique is highly controllable and can achieve large increases in leakage inductance; however, the transformer becomes larger, heavier, and more expensive. Sector winding, as advanced in this paper, produces very large increases in the leakage inductance at virtually no added cost or weight. The method in [24] is applicable for relatively small leakage inductance gains, say for a target increase of up to five times the natural (or minimum) leakage inductance  $L_0$ . The method promoted in this paper will find applications when the desired leakage inductance is several orders of magnitude larger than the natural value.

Recently, in [25] a turn-by-turn formulation to compute the leakage inductance in common-mode chokes was presented. A rectangular turn is broken into four straight line conductors and approximate solutions on infinitely long geometries are used for

Manuscript received November 22, 2012; revised February 5, 2013; accepted March 2, 2013. Date of current version July 18, 2013. This work was supported by the U.S. Department of Energy under Grant DEOE0000072. Recommended for publication by Associate Editor C. R. Sullivan.

F. de León is with the Department of Electrical and Computer Engineering, Polytechnic Institute of New York University, Brooklyn, NY 11201 USA (e-mail: fdeleon@poly.edu).

S. Purushothaman is with FM Global Research, Norwood, MA 02062 USA (e-mail: sujitp@ieee.org).

L. Qaseer is with the Al-Khwarizmi College of Engineering, University of Baghdad, Baghdad, Iraq (e-mail: laythqaseer@yahoo.com).

Color versions of one or more of the figures in this paper are available online at <http://ieeexplore.ieee.org>.

Digital Object Identifier 10.1109/TPEL.2013.2251429

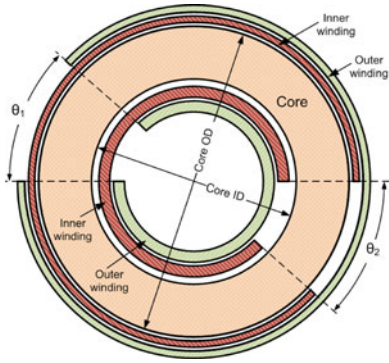


Fig. 1. Toroidal transformer with sectored windings.

each region. Thus, the inner conductor is modeled as an eccentric conductor inside of a ferromagnetic cylinder. Similarly, the outer conductor is represented as being outside the ferromagnetic cylinder. The lateral conductors are considered as filamentary currents on top of an infinite ferromagnetic plane with the method of images. The method in [25] is applicable to toroids with a few thick turns that can be wound in only one layer (for example, common-mode chokes), but it is not applicable to multilayer transformers. The frequency dependence is considered by including the resistances and the capacitances producing a wide-band circuitual model. Previously, in [26] a method to measure the leakage inductance of multiwinding chokes was presented. A model to describe the terminal behavior is given, but there are no equations to compute the parameters from dimensions.

There are two objectives of this paper: first is to present a methodology to increase the leakage inductance of toroidal transformers by leaving unwound sectors in the windings (see Fig. 1). Second is to propose an equation for the calculation of the leakage inductance suitable for a design program.

Although toroidal transformer manufacturers know that leaving unwound sectors increases the leakage inductance, the desired leakage inductance value is obtained by trial and error. In this paper, the transformer leakage inductance is expressed as a function of the number of turns  $N$ , the geometrical dimensions of the toroidal transformer, internal diameter ID, external diameter OD, height HT, and the angle of the unwound sector  $\theta$ .

This paper deals with a wide range of power transformer sizes of rectangular cross-sectional area. The core dimensions cover the following range: height from 1 to 6 in; external diameter from 4 to 13 in; and internal diameter from 1 to 10 in. These combinations cover most of the power conditioning application today from 1 kVA to perhaps 100 kVA (depending on the switching frequency). We have only experimented with unwound sector angles from  $30^\circ$  to  $180^\circ$ . It is quite possible, however, that the equations of this paper are applicable to much larger transformers with larger unwound angles. A few numerical experiments shown later indicate this, but more research is needed to make stronger claims.

The formula proposed in this paper is obtained from the observation of the behavior of the leakage inductance when the construction parameters of toroidal transformers are varied. More than 400 3-D FEM (finite elements) simulations have been performed to cover a very wide range of applications. Over 20 prototypes were built to validate the FEM simulations and the proposed formula.

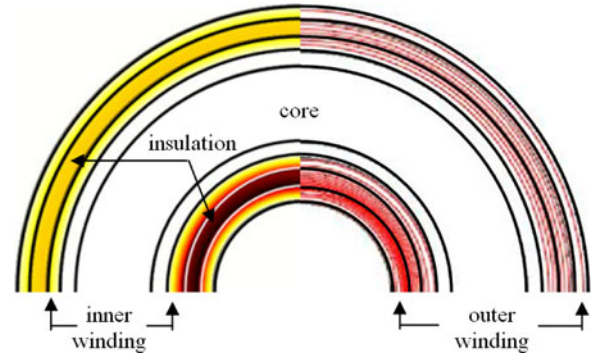


Fig. 2. Axial view of a toroidal transformer with windings covering  $360^\circ$ . The left-hand quadrant shows the surface plot of the distribution of the magnetic flux density while the right-hand quadrant shows the direction of the streamlines (concentric circles).

## II. THEORETICAL CONSIDERATIONS

To make the presentation accessible to wider audiences and to establish the nomenclature, we start by presenting the basic concepts of leakage flux for toroidal transformers. Two geometrical arrangements are discussed: toroidal transformers that are wound around  $360^\circ$  and toroids with sectored windings. Leakage flux is defined for a pair of windings as the flux that links only one winding and does not link the other winding. The corresponding leakage inductance is obtained in the laboratory through the SC test, which consists of feeding a winding with rated current when the other winding has its terminals short-circuited. The test can be simulated with FEM to obtain the leakage inductance. Additionally, with simulations one can fully eliminate any influence from the magnetizing current, while the SC test does not fully cancel the magnetizing flux.

### A. Toroidal Transformers With $360^\circ$ Windings

The leakage flux in a toroidal transformer, whose windings are one on top of the other for the entire  $360^\circ$ , is produced by the current in the windings that are equal in magnitude (i.e.,  $N_1 I_1 = N_2 I_2$ ), but opposite in direction. By forcing  $N_1 I_1 = N_2 I_2$ , there is no (magnetizing or leakage) flux in the core. As shown in Fig. 2, the leakage flux does not start nor it ends in the core, but closes in itself. The left-hand quadrant shows the surface plot of the distribution of the magnetic flux density while the right-hand quadrant shows the direction of the streamlines (concentric circles). Note that most of the leakage flux is in the insulation between the windings; some flux is also present in the windings, but there is no flux outside the region occupied by the windings. The leakage inductance for such geometry is computed in [24] from the energy stored yielding

$$L_0 = \frac{N^2 \mu_0}{2\pi} \sum_{i=1}^5 \eta_i (\alpha_i a + \phi_i g + \beta_i b) \quad (1)$$

where variables  $\eta_i$ ,  $\alpha_i$ ,  $\beta_i$ , and  $\phi_i$  are computed from the radii of the windings and include the factors of partial linkage fluxes in the windings; and  $a$ ,  $b$ , and  $g$  are the thicknesses of the inner winding, the outer winding, and the insulation layers, respectively; all the details are given in the Appendix.

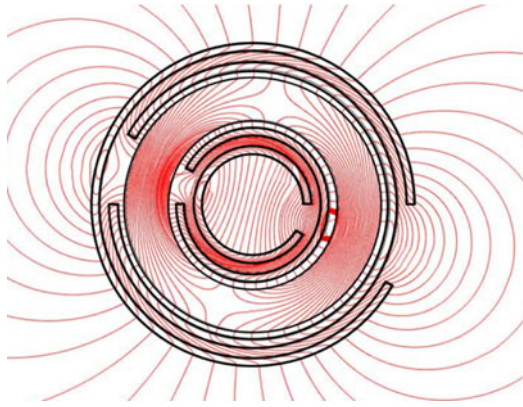


Fig. 3. Top view of the distribution of the leakage flux in a sectored wound transformer.

### B. Sectored Wound Toroidal Transformers

In sectored wound transformers, i.e., when the windings do not cover the entire  $360^\circ$ , the leakage flux follows a completely different path. Fig. 3 shows the top view of the leakage flux distribution. One can see that in this case the path of the leakage flux includes a section of the core. The amount of leakage flux that a winding links depends on the sector that is not wound. From Fig. 3, it is possible to see that many lines of flux only partially link the winding. We make the remark that the shape of the leakage flux does not change significantly as the angle of the wound sector varies. However, the intensity of the leakage flux increases substantially as the unwound angle increases. It should be mentioned that the flux in the core contributes very little to the leakage inductance since the energy stored depends on the square of the magnetic field strength  $H$ , which is very small in the core due to its high permeability.

### III. INITIAL EXPERIMENTATION

A first set of prototypes were built consisting of 7.25 kVA transformers  $V_1 = 215$  V and  $V_2 = 1928$  V. These transformers are used in a pulse width modulation application to drive a sonar amplifier. A standard toroidal transformer design for the specified power and voltage levels has a leakage inductance of under  $10 \mu\text{H}$ . For those conditions, an external series inductor of around  $800 \mu\text{H}$  is needed to help filtering the input of the amplifier at 450 Hz. Alternatively, we designed a transformer with increased leakage inductance. The transformer parameters are  $N_1 = 97$  turns and  $N_2 = 870$  turns. The core dimensions are  $\text{OD} = 175$  mm,  $\text{ID} = 100$  mm, and  $\text{HT} = 45$  mm.

Table I shows the total leakage inductance, referred to the low voltage side ( $N = 97$ ), of a set of prototypes built with equal unwound sectors in both windings, but displaced  $180^\circ$ ; see Fig. 4. As a reference, note that the magnetizing inductance of these toroidal transformers is about 1 H, which is much larger than the natural inductance of  $L_0 = 9.3 \mu\text{H}$  (for  $\theta = 0^\circ$ ) and even substantially larger than the largest leakage of 2.6 mH which we measured resulting from sectored windings (for  $\theta = 180^\circ$ ).

Fig. 5 shows the variation of the leakage inductance with respect to the unwound angle, which seems to be perfectly quadratic. Therefore, added to the plot of Fig. 5 there is a fitted quadratic equation of the form

$$L = K\theta^2. \quad (2)$$

TABLE I  
MEASURED LEAKAGE INDUCTANCE VERSUS UNWOUND ANGLE

| Point | Angle $\theta_1 = \theta_2$<br>[Degrees] | $L$ (measured)<br>[ $\mu\text{H}$ ] $N=97$ |
|-------|--|--|
| 0     | 0  | $L_0 = 9.3$                                |
| 1     | 15                                       | 17.6                                       |
| 2     | 30                                       | 56.7                                       |
| 3     | 45                                       | 151  |
| 4     | 65                                       | 320  |
| 5     | 80                                       | 499  |
| 6     | 100                                      | 777  |
| 7     | 120                                      | 1032                                       |
| 8     | 180                                      | 2600                                       |

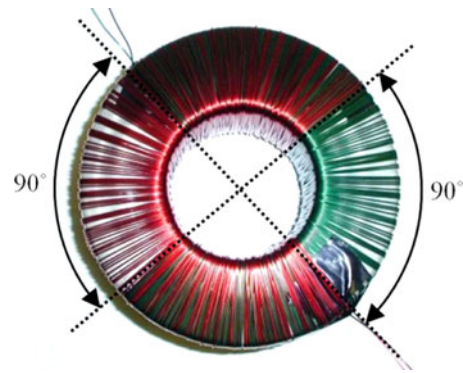


Fig. 4. Toroidal transformer with  $90^\circ$  sectored windings displaced  $180^\circ$ .

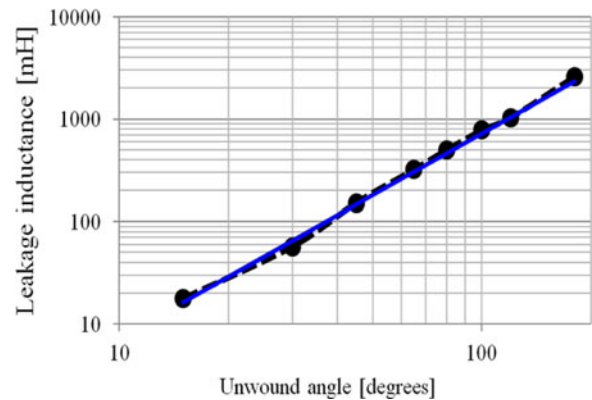


Fig. 5. Fitting a quadratic function to the experimental data.

For this example,  $K = 7.203 \times 10^{-2}$  when the unwound angle  $\theta$  is given in degrees and  $L$  in  $\mu\text{H}$ .

It is difficult to control the interturn spacing with high-speed winding machines and overlapping frequently occurs. However, “messy” windings when are elements of a sector winding strategy have relatively little effect in the leakage inductance (provided that they cover certain angle). A few experiments using “bank winding,” which consists in purposely producing overlapping by changing the rotation direction of the rollers, show very little increase in the leakage inductance. However, to obtain consistent leakage inductance values, it is important to precisely control the unwound angle. For this, a physical barrier beyond which the winding cannot pass is used.



TABLE II  
LEAKAGE INDUCTANCE COMPARISON BETWEEN FEM AND SC TESTS ON  
PROTOTYPES WITH  $N = 400$

| No | Core Dimensions [inch] |    |    | Angle $\theta$<br>[deg] | $L_0$<br>[mH] | FEM $L$<br>[mH] | SC test $L$<br>[mH] | %<br>difference |
|----|------------------------|----|----|-------------------------|---------------|-----------------|---------------------|-----------------|
|    | OD                     | ID | HT |                         |               |                 |                     |                 |
| 1  | 10                     | 8  | 2  | 180                     | 0.322         | 42.71           | 45.27               | -5.64           |
| 2  | 10                     | 6  | 2  | 180                     | 0.287         | 47.25           | 52.6                | -10.17          |
| 3  | 10                     | 4  | 2  | 180                     | 0.252         | 51.40           | 53.14               | -3.27           |
| 4  | 8                      | 4  | 2  | 180                     | 0.215         | 42.18           | 42.27               | -0.21           |
| 5  | 6                      | 4  | 2  | 180                     | 0.179         | 32.72           | 36.65               | -10.72          |
| 6  | 6                      | 4  | 3  | 180                     | 0.115         | 38.85           | 39.28               | -1.10           |
| 7  | 6                      | 4  | 1  | 180                     | 0.363         | 26.24           | 28.11               | -6.64           |
| 8  | 6                      | 4  | 1  | 150                     | 0.363         | 17.34           | 18.6                | -6.78           |
| 9  | 6                      | 4  | 1  | 110                     | 0.363         | 8.80            | 9.14                | -3.72           |
| 10 | 6                      | 4  | 1  | 90                      | 0.363         | 5.75            | 5.67                | 1.48            |
| 11 | 6                      | 4  | 1  | 40                      | 0.363         | 1.15            | 1.08                | 6.88            |

#### IV. SYSTEMATIC EXPERIMENTATION

A set of 11 prototypes was built with the purpose of shedding light on the parameters influencing the value of  $K$ . This set, in addition to varying the unwound sector, also included variation of other geometric parameters of the core, i.e., ID, OD, and HT. Table II gives the geometric details of the prototypes along with the leakage inductance obtained in the laboratory with SC test. Measurements with an LCR meter (at 60 Hz) confirmed the results of the SC tests. In Table II, the value of  $L_0$  has been added as reference. One can appreciate that  $L_0$  is negligible for unwound angles of  $90^\circ$  or larger. Prototypes 1, 2, and 3 have all parameters but ID constant. These three prototypes can be used to study the effect of ID on the leakage reactance. Similarly, prototypes 3, 4, and 5 can be used to study the effect of the variation of OD on the transformer leakage. Height variations can be studied with prototypes 5, 6, and 7. All prototypes have 400 turns on each winding.

Although we found very little effect on the core losses at 60 Hz due to sector winding, it has been found in [27] that the core losses increase considerably due to the orthogonal flux in cut tape-wound cores at high frequencies. Although the techniques of this paper are directly applicable to ferrite cores over a wide frequency range, further investigation is needed to gauge the effect on losses for uncut tape-wound cores at high frequencies.

Measurements with the LCR meter at 1 kHz show an average reduction in the leakage inductance of about 12% from the value at 60 Hz; the larger the transformer, the larger the reduction. Further research will be carried out to model the frequency dependence of the leakage inductance in sector winding toroidal transformers.

#### V. FEM SIMULATIONS

Three-dimensional (3-D) finite element simulations are performed to generate additional cases needed for the derivation of a mathematical model. The leakage inductance is computed from the total energy stored in the magnetostatic field when one winding is fed with unity current in one direction and the second is fed with unity current in the opposite direction. This effectively eliminates any effect of the magnetizing current since

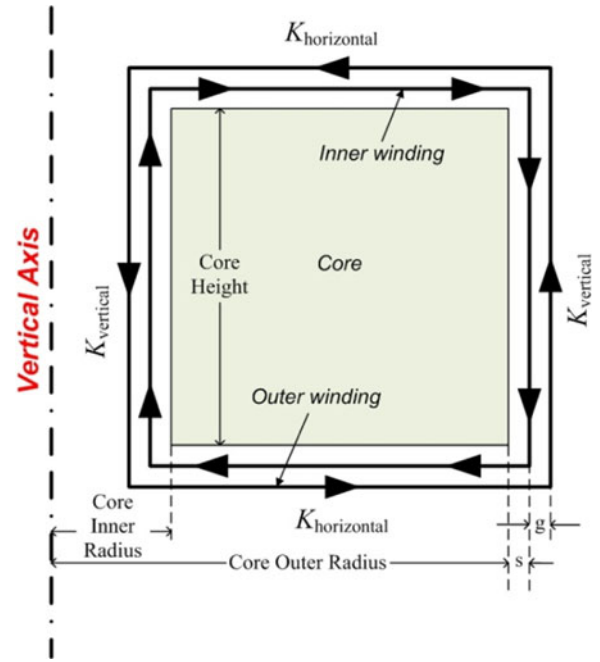


Fig. 6. Cross section of the FEM model.

$N_1 I_1 = N_2 I_2$  is strictly enforced. A total of 420 different transformer configurations were analyzed with 3-D FEM simulations.

Even though the toroidal core is symmetric around the central axis, the windings are not. Each winding exists for  $360^\circ - \theta^\circ$  around the central axis as shown in Fig. 1; moreover, the core height is not infinite in depth. Hence, an axisymmetric or a two-dimensional (2-D) model cannot be used to represent a sector wound toroidal transformer.

The windings are modeled as thin sheets carrying currents in the opposite direction to simulate the conditions of the SC test needed to measure the leakage inductance. The windings were initially modeled as volume regions with finite thickness having an impressed current density  $J$ , but it was found from many experiments that the coil thickness played only a minor role in the leakage inductance when there is an unwound sector of at least  $30^\circ$ . Hence, the optimum FEM simulations use a current sheet to represent the windings. A cross section of the FEM model is presented in Fig. 6. It must be noted that such a 3-D model consists of 100 000 to 200 000 second-order finite elements and takes 30 min to solve using a server that has 24 cores in its CPU running at 3.33 GHz each as well as 96 GB of DDR3 RAM.

Table II shows the comparison between the experimental results and the corresponding 3-D FEM simulations. One can appreciate that the simulations yield very good results when compared to the experiments. The small differences are attributed to manufacturing tolerances in the prototypes. Fig. 7 shows cuts of the front and top views of the distribution of the magnetic flux density.

The surface current densities  $K_{vertical}$  and  $K_{horizontal}$  are chosen such that the total current is the same ( $N_1 I_1 = N_2 I_2$ ). While  $K_{horizontal}$  is a function of spatial coordinates,  $K_{vertical}$  is constant in magnitude and is not a function of spatial coordinates. In a completely wound ( $\theta = 0^\circ$ ) transformer, the leakage

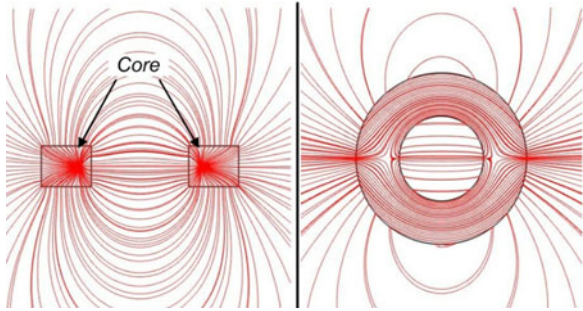


Fig. 7. FEM flux density streamline plot. (a) Front view. (b) Top view.

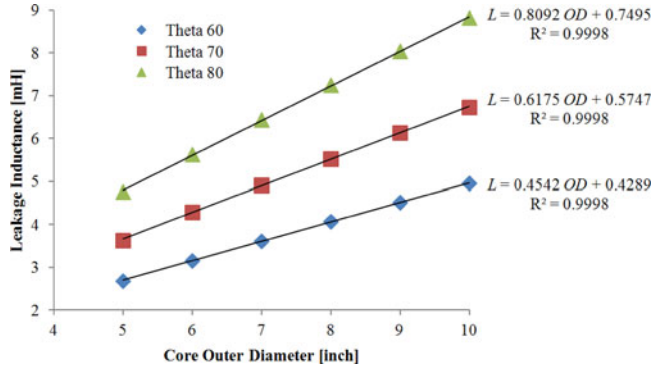


Fig. 8. Variation of leakage inductance with core outer diameter. The dots correspond to the simulated values. The trend lines and their equations are also presented.

flux flows through the interwinding gap  $g$  and hence is a critical factor contributing in the leakage inductance; see [24]. In a sector-wound transformer, the leakage flux is dictated by  $\theta$ , ID, OD, and HT.

## VI. MATHEMATICAL MODEL

The validation of the FEM simulations against experimental results, as shown in Table II, enables the derivation of a mathematical formula for the calculation of the leakage inductance of sector-wound toroidal transformers based on the results of FEM simulations. In this section, a double regression method is employed to obtain a simple formula for the leakage inductance.

From numerous tests on transformers having the same number of primary and secondary turns of 400, it was found that there exists a linear relationship between the leakage inductance  $L$  and the outer diameter of the core OD. This can be written in the following form:

$$L = b_{10} + \beta_1 OD \quad (3)$$

where  $L$  is the leakage inductance and  $\beta_1$  is the contribution factor for the outer diameter. Fig. 8 shows the relationship between the leakage inductance and the outer diameter, keeping all other parameters fixed (ID = 4", HT = 2"). Results are plotted for (unwound) sector angles of 60°, 70°, and 80°.

Fig. 9 shows the relationship between the leakage inductance and the inner diameter ID when keeping the other parameters fixed (OD = 10", HT = 2"). Results are plotted for sector angles of 60°, 70°, and 80°. It can be seen from Fig. 9 that the leakage inductance varies linearly in inverse proportion to the inner core

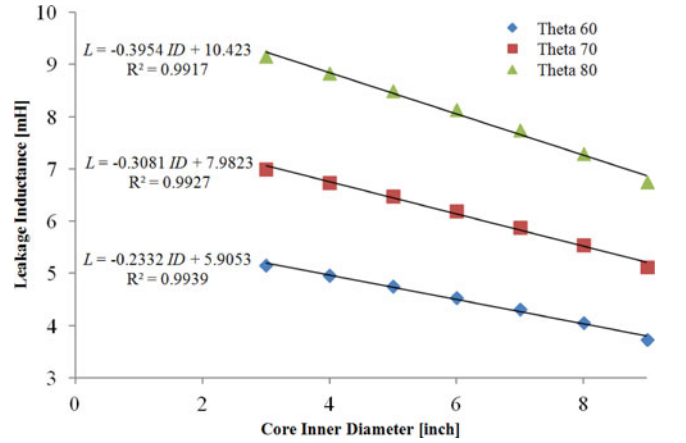


Fig. 9. Variation of leakage inductance with core inner diameter. The dots correspond to the simulated values. The trend lines and their equations are also presented.

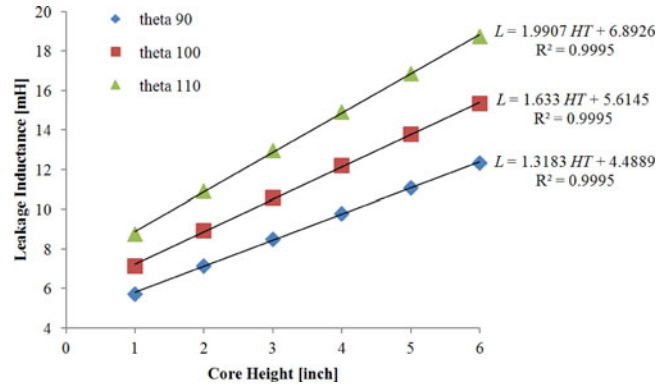


Fig. 10. Variation of leakage inductance with core height. The dots correspond to the simulated values. The trend lines and their equations are also presented.

diameter ID, which can be expressed as

$$L = b_{20} + \beta_2 ID \quad (4)$$

where  $\beta_2$  is the contribution factor for the inner diameter.

We have also observed that the leakage inductance varies linearly with core height HT as

$$L = b_{30} + \beta_3 HT \quad (5)$$

where  $\beta_3$  is the contribution factor for core height. Fig. 10 shows the relationship between the leakage inductance and the core height when keeping all other parameters fixed (OD = 6", ID = 4"), for sector angles of 90°, 100°, and 110°.

Finally, we note that the leakage inductance varies with the unwound sector angle as a quadratic function. This is given as

$$L = b_{40} + c_1 \theta^2 \quad (6)$$

where  $\theta$  is the sector angle in radians. Fig. 11 shows the relationship between the leakage inductance and the unwound sector angle for a transformer keeping other parameters fixed (OD = 6", ID = 4"). Results are plotted for three cases with core height = 2", 3", and 4". The sector angle is varied from 10° to 350° to cover the entire spectrum. The slope  $m = 2$  of the lines in the log-log plot confirms the quadratic variation.

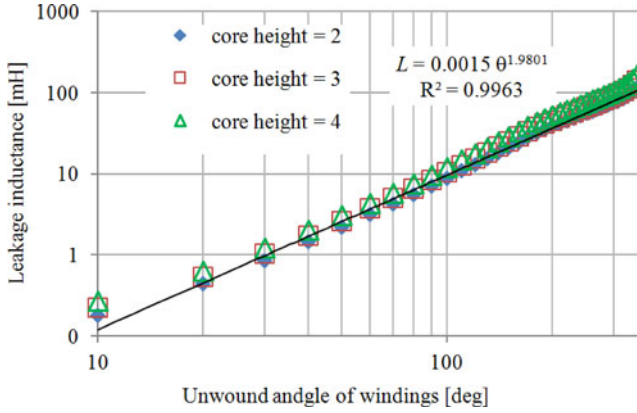


Fig. 11. Variation of leakage inductance with unwound sector winding angle. The dots correspond to the simulated values. The trend line for core height = 3 in and its equation is also presented.

Consistent with theory, all analytical formulas for the calculation of inductances reveal that they depend on the square of the number of turns. Combing (3)–(6) into a single equation gives an inductance formula as a function of the inner diameter, outer diameter, core height, sector winding angle, and the number of turns as follows:

$$L = L_0 + \mu_0 N^2 (\beta_1 OD + \beta_2 ID + \beta_3 HT) \quad (7)$$

where  $L_0$  is the leakage inductance for a transformer with complete  $360^\circ$  windings or sector angle of  $0^\circ$ . The procedure to evaluate  $L_0$  has been given in [24] and reproduced in the Appendix.

Exhaustive analysis of the numerical results has yielded that the contribution factors  $\beta_i$  are quadratic functions of the sector angle  $\theta$  as follows:

$$\begin{aligned} \beta_1 &= k_1 \theta^2 \\ \beta_2 &= k_2 \theta^2 \\ \beta_3 &= k_3 \theta^2. \end{aligned} \quad (8)$$

Here,  $\beta_1$ ,  $\beta_2$ , and  $\beta_3$  correspond to the slopes of the lines of Figs. 8–10, respectively. Hence, (7) simplifies to

$$L = L_0 + \mu_0 N^2 (k_1 OD + k_2 ID + k_3 HT) \theta^2 \quad (9)$$

where OD, ID, and HT are given in inches,  $\theta$  is in degrees, and  $L$  is in milli-Henry. The thickness of the windings  $a$  and  $b$  in (1) only affects  $L_0$ .

The values of  $k_1$ ,  $k_2$ , and  $k_3$  in (9) are evaluated by a two-step regression readily available in Excel. Multiple cases are generated using the FEM model described in Section V. The geometric parameters ID, OD, and HT are varied in steps for every sector angle  $\theta$ .

A linear regression is first performed on data with constant  $\theta$  and the values of  $\beta_1$ ,  $\beta_2$ , and  $\beta_3$  are evaluated. This is repeated for various values of sector angle  $\theta$ , yielding different values of  $\beta_i$ . 210 cases of the 420 cases generated by the FEM model were used. It must be noted that the coefficient of determination  $R^2$  is larger than 99% for all the cases, indicating an excellent fit. Fig. 12 shows the variation of  $\beta_i$  with respect to the square of the sector angle.

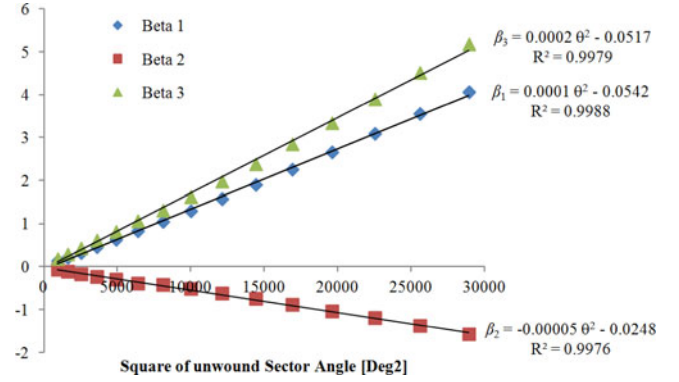


Fig. 12. Variation of  $\beta_i$  with unwound sector winding angle. The dots correspond to the simulated values. The trend lines and their equations are also presented.

Fig. 12 confirms the quadratic variation of  $\beta_i$  with sector angle given in (8). The second regression is performed on the data plotted in Fig. 12 to satisfy (8) yielding the values of  $k_i$  as follows:

| Units for OD, ID, HT | $k_1$                   | $k_2$                    | $k_3$                   |
|----------------------|-------------------------|--------------------------|-------------------------|
| mm                   | $2.6444 \times 10^{-5}$ | $-1.104 \times 10^{-5}$  | $3.178 \times 10^{-5}$  |
| inch                 | $6.7168 \times 10^{-4}$ | $-2.8043 \times 10^{-4}$ | $8.0723 \times 10^{-4}$ |

Here,  $k_1$ ,  $k_2$ , and  $k_3$  are the contributing factors of the geometric parameters of the core OD, ID, and HT, respectively. When the geometric dimensions of the transformer are given in millimeters,  $k_1$ ,  $k_2$ , and  $k_3$  have units of  $\text{deg}^{-2}$ .

The double regression used in this paper (to model the leakage inductance for sectored winding transformers) gives a good balance between simplicity and accuracy. Equation (9) is very simple, yet sufficiently accurate for engineering design. We have investigated the effects of fitting curves for other variables and ratios. For example, it was experimented with ratios of OD/ID, differences (OD-ID), compound ratios as (OD-ID)/(OD+ID), and their powers (squares and roots). Slightly more accurate results can be obtained with some combinations; however, the resulting equations are substantially more intricate than (9).

## VII. RESULTS

Table III presents the comparison between 24 of the close to 250 cases used for the validation of the proposed model against FEM simulations. These cases are provided to cover a wide range of core dimensions. For each set of OD, ID, and HT, the unwound sector angle  $\theta$  is set to  $60^\circ$ ,  $120^\circ$ , and  $240^\circ$ . Most of the results match very well. It was observed that transformers with cross-sectional area close to a square aspect ratio ( $HT \cong (OD-ID)/2$ ) have errors smaller than 5%. Tall and flat looking transformers have errors smaller than 10%. If there are no special constraints on dimensions, square aspect ratio is preferred because the turn length is shorter. The value of  $L_0$  has been included in Table III. One can appreciate that  $L_0$  in all these cases is negligible, but this is not always the case. For smaller angles, say up to  $60^\circ$ ,  $L_0$  may play a role. Note that the values presented in Table III do not match with the same degree of accuracy as the cases used to fit the equations (as presented in Figs. 8–12).

TABLE III  
COMPARISON BETWEEN FEM AND PROPOSED MODEL (9)

| No | Core Dimensions [inch] |    |    | Unwound Angle $\theta$ [deg] | L[mH]  |           |                               |           | % difference |
|----|------------------------|----|----|------------------------------|--------|-----------|-------------------------------|-----------|--------------|
|    | OD                     | ID | HT |                              | FEM    | $L_0$ (1) | Sector Model $L - L_0$ in (9) | Total (9) |              |
| 1  | 4                      | 1  | 1  | 60                           | 2.48   | 0.049753  | 2.33                          | 2.380     | 6.05         |
| 2  |                        |    |    | 120                          | 9.11   | 0.049753  | 9.30                          | 9.350     | -2.09        |
| 3  |                        |    |    | 240                          | 35.19  | 0.049753  | 37.22                         | 37.270    | -5.77        |
| 4  |                        |    | 4  | 60                           | 4.57   | 0.003843  | 4.08                          | 4.084     | 10.72        |
| 5  |                        |    |    | 120                          | 16.01  | 0.003843  | 16.32                         | 16.324    | -1.94        |
| 6  |                        |    |    | 240                          | 61.30  | 0.003843  | 65.26                         | 65.264    | -6.46        |
| 7  |                        | 3  | 1  | 60                           | 1.88   | 0.068701  | 1.92                          | 1.989     | -2.13        |
| 8  |                        |    |    | 120                          | 7.59   | 0.068701  | 7.68                          | 7.749     | -1.19        |
| 9  |                        |    |    | 240                          | 29.91  | 0.068701  | 30.72                         | 30.789    | -2.71        |
| 10 |                        |    | 4  | 60                           | 3.76   | 0.011310  | 3.67                          | 3.681     | 2.39         |
| 11 |                        |    |    | 120                          | 14.63  | 0.011310  | 14.69                         | 14.701    | -0.41        |
| 12 |                        |    |    | 240                          | 57.43  | 0.011310  | 58.77                         | 58.781    | -2.33        |
| 13 | 12                     | 4  | 2  | 60                           | 5.91   | 0.079918  | 6.19                          | 6.270     | -4.74        |
| 14 |                        |    |    | 120                          | 24.30  | 0.079918  | 24.76                         | 24.840    | -1.89        |
| 15 |                        |    |    | 240                          | 94.87  | 0.079918  | 99.05                         | 99.130    | -4.41        |
| 16 |                        |    | 6  | 60                           | 8.46   | 0.023534  | 8.53                          | 8.554     | -0.83        |
| 17 |                        |    |    | 120                          | 34.28  | 0.023534  | 34.11                         | 34.134    | 0.50         |
| 18 |                        |    |    | 240                          | 132.32 | 0.023534  | 136.45                        | 136.474   | -3.12        |
| 19 |                        | 9  | 2  | 60                           | 4.78   | 0.101876  | 5.18                          | 5.282     | -8.37        |
| 20 |                        |    |    | 120                          | 20.20  | 0.101876  | 20.70                         | 20.802    | -2.48        |
| 21 |                        |    |    | 240                          | 79.03  | 0.101876  | 82.81                         | 82.912    | -4.78        |
| 22 |                        |    | 6  | 60                           | 7.32   | 0.032882  | 7.51                          | 7.543     | -2.60        |
| 23 |                        |    |    | 120                          | 30.37  | 0.032882  | 30.05                         | 30.083    | 1.05         |
| 24 |                        |    |    | 240                          | 117.49 | 0.032882  | 120.21                        | 120.243   | -2.32        |

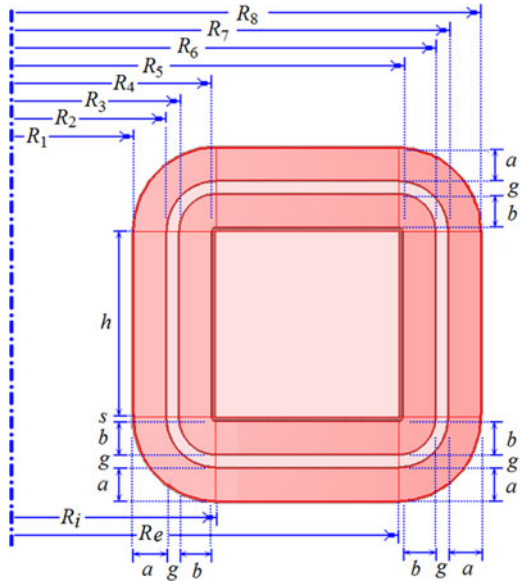


Fig. 13. Definition of variables for (11).

This is so because Table III gives the extremes used to validate the model; these cases represent the worst case scenarios.

To gauge the validity of the formulas for large transformers, a set of FEM simulations for unrealistically large transformers were performed. We used OD = 6 m, ID = 4 m, and HT =

1 m for unwound angles of 60°, 120°, 240°, and 270°. We found differences between FEM and (9) of only -6.80%, -1.56%, -2.08%, and -6.58%, respectively.

## VIII. CONCLUSION

A methodological technique to increase considerably the leakage inductance of power toroidal transformers by leaving unwound sectors has been developed. Additionally, a formula to

TABLE IV  
COEFFICIENTS FOR THE DIFFERENT COMPONENTS OF THE LEAKAGE INDUCTANCE FORMULA GIVEN IN (1)

| Section | Coefficient                     |                         |                          |                         |
|---------|---------------------------------|-------------------------|--------------------------|-------------------------|
|         | $\eta_i$                        | $\alpha_i$              | $\phi_i$                 | $\beta_i$               |
| 1       | $h$                             | $\frac{R_{m1}}{3R_2^2}$ | $\frac{R_{m2}}{2R_2R_3}$ | $\frac{R_{m3}}{3R_3^2}$ |
| 2       | $h$                             | $\frac{R_{m7}}{3R_7^2}$ | $\frac{R_{m6}}{2R_6R_7}$ | $\frac{R_{m5}}{3R_6^2}$ |
| 3       | $\frac{R_e^2 - R_i^2}{R_e R_i}$ | $\frac{1}{3}$           | 1                        | $\frac{1}{3}$           |
| 4       | $\frac{1}{2R_2^2}$              | $\frac{R_{m1}t_1}{6}$   | $R_{m2}t_2$              | $\frac{R_{m3}t_3}{6}$   |
| 5       | $\frac{1}{2R_6^2}$              | $\frac{R_{m7}t_1}{6}$   | $R_{m6}t_2$              | $\frac{R_{m5}t_3}{6}$   |



compute the leakage inductance for sectored wound transformers has been derived from the observation of its behavior through hundreds of 3-D FEM simulations. The leakage inductance is computed with a simple formula from the physical quantities of the transformer: number of turns and core dimensions—internal and external diameter, height, and the angle of the unwound sector. Therefore, the equation is suitable for implementation in transformer design programs or even hand calculations. The FEM simulations and the formula have been corroborated experimentally with over 20 prototypes of varied sizes and winding conditions.

## APPENDIX

### CALCULATION OF $L_0$

In this section, the necessary information to compute  $L_0$  using (1) is reproduced from [24]. The geometrical arrangement and the definition of all variables are given in Fig. 13. The coefficients  $\eta_i$ ,  $\alpha_i$ ,  $\beta_i$ , and  $\phi_i$  for the different sections are given in Table IV. The following relationships are needed to complete the information:

$$R_{m,j} = (R_j + R_{j+1})/2 \quad (11a)$$

$$t_1 = 3a + 4(s + b + g) \quad (11b)$$

$$t_2 = g + 2(s + b) \quad (11c)$$

$$t_3 = 3b + 4s. \quad (11d)$$

### ACKNOWLEDGMENT

The first author would like to thank the people (coworkers and students) who have worked with him in this project over the past 12 years; in chronological order: V. Tatu, S. Magdaleno, I. Hernandez, N. Augustine, and C. Prabhu.

### REFERENCES

- [1] J. O. Krah and J. Holtz, "Total compensation of line-side switching harmonics in converter-fed AC locomotives," *IEEE Trans. Ind. Appl.*, vol. 31, no. 6, pp. 1264–1273, Nov./Dec. 1995.
- [2] S. Saetio, R. Devaraj, and D. Torrey, "The design and implementation of a three-phase active power filter based on sliding mode control," *IEEE Trans. Ind. Appl.*, vol. 31, no. 5, pp. 993–1000, Sep./Oct. 1995.
- [3] N. Kutkut, D. Divan, and R. Gascoigne, "An improved full-bridge zero-voltage switching PWM converter using a two-inductor rectifier," *IEEE Trans. Ind. Appl.*, vol. 31, no. 1, pp. 119–126, Jan./Feb. 1995.
- [4] M. Kheraluwala, R. Gascoigne, D. Divan, and E. Baumann, "Performance characterization of a high-power dual active bridge dc-to-dc converter," *IEEE Trans. Ind. Appl.*, vol. 28, no. 6, pp. 1294–1301, Nov./Dec. 1992.
- [5] A. Yagasaki, "Highly improved performance of a noise isolation transformer by a thin-film short-circuit ring," *IEEE Trans. Electromagn. Compat.*, vol. 41, no. 3, pp. 246–250, Aug. 1999.
- [6] S. Ogasawara, H. Ayano, and H. Akagi, "An active circuit for cancellation of common-mode voltage generated by PWM inverter," *IEEE Trans. Power Electron.*, vol. 13, no. 5, pp. 835–841, Sep. 1998.
- [7] T. Yanada, S. Minowa, O. Ichinokura, and S. Kikuchi, "Design and analysis of noise-reduction transformer based on equivalent circuit," *IEEE Trans. Magnet.*, vol. 34, no. 4, pp. 1351–1353, Jul. 1998.
- [8] T. Yanada and O. Ichinokura, "High performance step-down noise-reduction transformer constructed with C-core," *IEEE Trans. Magnet.*, vol. 33, no. 5, pp. 3331–3333, Sep. 1997.
- [9] S. Ogasawara and H. Akagi, "Modeling and damping of high-frequency leakage currents in PWM inverted-Fed AC motor drive systems," *IEEE Trans. Ind. Appl.*, vol. 32, no. 5, pp. 1105–1114, Sep./Oct. 1996.
- [10] F. Forest, E. Laboure, T. A. Meynard, and V. Smet, "Design and comparison of inductors and intercell transformers for filtering of PWM inverter output," *IEEE Trans. Power Electron.*, vol. 24, no. 3, pp. 812–821, Mar. 2009.
- [11] *IEEE Recommended Practice for Protection and Coordination of Industrial and Commercial Power Systems*, IEEE Standard 242-1986, Feb. 1986.
- [12] Plitron Manufacturing Inc., "Toroidal transformer catalog," (2012). [Online]. Available: www.plitron.com
- [13] W. T. McLymann, *Transformer and Inductor Design Handbook*. New York, NY, USA: Marcel Dekker, 1998.
- [14] K. Karsai, D. Kerényi, and L. Kiss, *Large Power Transformers*. Amsterdam, The Netherlands: Elsevier, 1987, p. 95.
- [15] G. Slemmon, *Electric Machines and Drives*. Reading, MA, USA: Addison-Wesley, 1992, pp. 252–255.
- [16] R. Stoll, *The Analysis of Eddy Currents*. Oxford, U.K.: Clarendon, 1974.
- [17] F. de León and A. Semlyen, "Time domain modeling of eddy current effects for transformer transients," *IEEE Trans. Power Deliv.*, vol. 8, no. 1, pp. 271–280, Jan. 1993.
- [18] K. W. E. Cheng and P. D. Evans, "Calculation of winding losses in high-frequency toroidal inductors using single strand conductors," in *IEE Proc. Elect. Power Appl.*, Mar. 1994, vol. 141, no. 2, pp. 52–62.
- [19] K. W. E. Cheng and P. D. Evans, "Calculation of winding losses in high frequency toroidal inductors using multistrand conductors," in *IEE Proc. Elect. Power Appl.*, Sep. 1995, vol. 141, no. 5, pp. 313–322.
- [20] R. Prieto, J. A. Cobos, V. Bataller, O. Garcia, and J. Uceda, "Study of toroidal transformers by means of 2D approaches," in *Proc. 28th Annu. IEEE Power Electron. Spec. Conf.*, Jun. 22–27, 1997, pp. 621–626.
- [21] R. Prieto, V. Bataller, J. A. Cobos, and J. Uceda, "Influence of the winding strategy in toroidal transformers," in *Proc. 24th Annu. Conf. IEEE Ind. Electron. Soc.*, Aug. 31–Sep. 4, 1998, pp. 359–364.
- [22] M. Nave, "On modeling the common mode inductor," in *Proc. IEEE Int. Symp. Electromagn. Compat.*, Aug. 1991, pp. 452–457.
- [23] W. G. Hurley and D. J. Wilcox, "Calculation of leakage inductance in transformer windings," *IEEE Trans. Power Electron.*, vol. 9, no. 1, pp. 121–126, Jan. 1994.
- [24] I. Hernández, F. de León, and P. Gómez, "Design formulas for the leakage inductance of toroidal distribution transformers," *IEEE Trans. Power Deliv.*, vol. 26, no. 4, pp. 2197–2204, Oct. 2011.
- [25] M. Kovacic, Z. Hanic, S. Stipetic, S. Krishnamurthy, and D. Zarko, "Analytical wideband model of a common-mode choke," *IEEE Trans. Power Electron.*, vol. 27, no. 7, pp. 3173–3185, Jul. 2012.
- [26] A. J. Binnie and T. R. Foord, "Leakage inductance and interwinding capacitance in toroidal ratio transformers," *IEEE Trans. Instrum. Meas.*, vol. 16, no. 4, pp. 307–314, Dec. 1967.
- [27] B. Cougo, A. Tuysüz, J. Muhlethaler, and J. W. Kolar, "Increase of tape wound core losses due to interlamination short circuits and orthogonal flux components," in *Proc. 37th Annu. Conf. IEEE Ind. Electron. Soc.*, Nov. 7–10, 2011, pp. 1372–1377.

**Francisco de León** (S'86–M'92–SM'02) received the B.Sc. and M.Sc. (Hons.) degrees in electrical engineering from the National Polytechnic Institute, Mexico City, Mexico, in 1983 and 1986, respectively, and the Ph.D. degree in electrical engineering from the University of Toronto, Toronto, ON, Canada, in 1992.

He has held several academic positions in Mexico and has worked for the Canadian electric industry. He is currently an Associate Professor at the Polytechnic Institute of New York University, Brooklyn, NY, USA. His research interests include the analysis of power definitions under nonsinusoidal conditions, the transient and steady-state analyses of power systems, the thermal rating of cables and transformers, and the calculation of electromagnetic fields applied to machine design and modeling.

**Sujit Purushothaman** (S'09–M'13) received the B.E. degree in electrical engineering from the Sardar Patel College of Engineering, Mumbai University, Mumbai, India, in 2005, and the Master's and Ph.D. degrees in electrical engineering from the Polytechnic Institute of New York University, Brooklyn, NY, USA, in 2009 and 2011, respectively.

He was involved in testing and development of medium-voltage switchgear for Siemens, Mumbai. He is currently a Research Engineer at FM Global Research, Norwood, MA, USA. His research interests include power system transients, damping of subsynchronous resonance, machine design and modeling, and thermal modeling of electrical devices.

**Layth Qaseer** received the B.Sc., M.Sc., and Ph.D. degrees from the University of Baghdad, Baghdad, Iraq, in 1979, 1993, and 2004, respectively, all in electrical engineering.

Between 1979 and 2001, he was with National Scientific Research Center and the Ministry of Industry. In 2005, he joined the Al-Khwarizmi College of Engineering, University of Baghdad. He was a Visiting Professor in the Department of Electrical and Computer Engineering, Polytechnic Institute of New York University, during the 2010–2011 academic year. His research interests include linear electric machines, electromagnetic systems, electrical machine design, permanent magnet synchronous motors, and modeling.